A Performance Analysis Technique of the Space-based SAR Processor Using RDA

In-Pyo Hong* *Regular Member*

ABSTRACT

It is an essential design process to analyze the performance of Synthetic Aperture Radar (SAR) processor before implementation. The contribution of this paper is to identify the chief sources and types of errors, to assess their impact on system performance, and to suggest the analysis technique for principal performance of the space-based SAR processor using Range-Doppler Algorithm (RDA). Also, simulation is performed by the Experimental-SAR (E-SAR) processor to examine the practicability and efficiency of the technique, the results are discussed, and solutions for the problems are recommended. Therefore, this technique can be used to analyze the performance of the space-based SAR processor using RDA.

Ⅰ. Introduction

Spaceborne SAR has found many important applications in remote sensing[1]. Then, spaceborne radar will participate in many remote sensing missions for observation of the earth and planets[2]. The SAR processor is the primary image generating component of the SAR system. Work during previous design stage set out the processing algorithm functional definitions. These definitions constitute the starting point of this paper. It is a critical design process to analyze the principal performance of the SAR processor at the detailed design stage.

Many previous papers have investigated not the overall performance analysis of the SAR processor but the specific point of view such as Doppler centroid estimation[3-5], processing speed[6,7], Secondary Range Compression (SRC)[8-10], Range Cell Migration (RCM)[11], etc. Some work has been published on comparisons between processing algorithms[12,13].

Thus, the contribution of this paper is to identify the chief sources of error and to suggest systematically the practical technique for overall performance analysis of the space-based SAR processor. Estimations of the magnitude of any errors are then made and summarized and their impact on the SAR system performance is assessed. The errors of SAR processor are due to imperfections in the algorithms selected or in their implementation. This paper focuses on not SAR system but SAR processor performance. Then, it is assumed that SAR system errors are already considered and included in the previous design stage.

Additionally, it is assumed a space-based SAR system for simulation and called the E-SAR, which is not a real but designed system based on the SAR system design criteria[1,14]. The simulation is performed to prove the practicability and efficiency of the technique.

Ⅱ. Performance Analysis Technique

RDA[15] is often chosen in a SAR processor because of its ability to compress a point target accurately, and because it can be implemented as a two one-dimensional matched filtering process.

This allows efficient computer implementation, and provides adequate accuracy control over key operations such as RCM correction[16]. Then, RDA

* 국방과학연구소(hip7777@hanmail.net)
논문번호 : 020218-0507, 접수일자 : 2002년 5월 7일

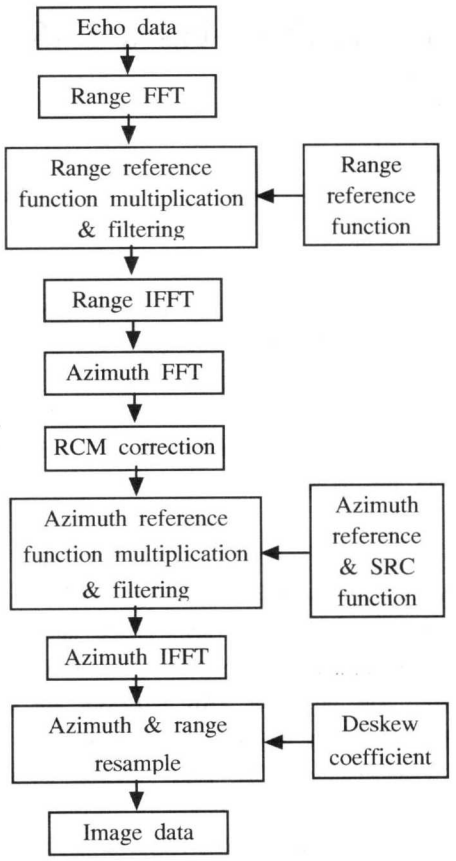

Fig. 1 Processing flow of the SAR processor using RDA

is selected for the performance analysis of the SAR processor. Fig. 1 illustrates the processing flow of RDA.

The space-based SAR processor using RDA may degrade image relative to an ideal SAR processor for the following reasons:

- The range and azimuth correlation filters are not quite matched at the main lobe location; assessed in terms of the quadratic phase error at the end of the aperture relative to the aperture center.
- The RCM correction is not sufficient than required.
- SAR processor adds noise like errors, random uncorrelated to image.
- Radiometric calibration is not consistent.
- Image location is not correctly calculated.

To analyze performance of SAR processor is to analyze errors of it. All errors can be classified by three kinds of error types such as azimuth focus, range focus, and noise type. Table 1 illustrates these error sources and types derived from the processing steps of echo data in Fig. 1. With the above contents, we can derive the processing error sources and their equations of the space-based SAR processor using RDA as following sections. These come from processing steps.

Table 1. Error sources and types for processing steps

Processing error sources	Error types			Remark
	Azimuth defocus	Range defocus	Noise type error	
BAQ decode			√	System error
Replica mismatch		√		System error
Range FFT & IFFT			√	
RCM correction - f_R mismatch - Interpolation error		√	 √	
Focus error due to f_R error - from orbit - from terrain height - from polynomial model - from azimuth block	 √ √ √ √			
Range Doppler dispersion		√		
Azimuth FFT & IFFT			√	
Azimuth deskew			√	
Range & azimuth interpolation error			√	
Calibration errors				System error(pixel magnitude error)
Location errors				Position error

2.1 Azimuth Defocus

1) Orbital Estimation Error

Orbit is assumed to be Keplerian[2,10]. Regression is fitted to Keplerian orbit. Orbital velocity that is found by assuming orbit eccentricity is known from previous observations. The orbital velocity is then related to the orbital radius since the gravitational acceleration is constant. Orbital acceleration is:

$$a = V^2 / R \tag{1}$$

$$\therefore \delta V = (V \delta R) / 2R \tag{2}$$

, where V is platform velocity and R is the distance from earth center to the platform. Doppler frequency modulation (f_R) is proportional to ($\sim$): $2V^2/\lambda R_s$, where λ is wavelength and R_s is slant range[17]. Therefore, f_R is $\sim (4V\delta V)/(\lambda R_s)$. Phase at the edge of aperture is:

$$\varphi = 0.5 f_R (\tau/2)^2 2\pi \quad (radians) \tag{3}$$

, where τ is synthetic aperture duration. Then, phase error at the edge of aperture is:

$$\delta\varphi = 0.5 \delta f_R (\tau/2)^2 360 \quad (^\circ). \tag{4}$$

2) Terrain Height Errors

To get the terrain height error, equation (1) is used:

$$a = V^2 / (d + k) \tag{5}$$

, where d is the radius of the earth at nadir and k is the SAR platform altitude to the nadir point. Component(a_L) in look direction is $\{V^2/(d+k)\}\cos\theta$, where θ is look angle. Error in target height h is error in θ and then it is $(h \sin i)/R_s$, where i is incidence angle. Therefore,

$$\delta a_L = \{V^2 / (d+k)\} \sin\theta \ \delta\theta = \{V^2 / (d+k)\} \sin\theta \ \{(h/R_s) \sin i\}. \tag{6}$$

Contribution to f_R is $(2\delta a_L)/\lambda$. Then,

$$\delta f_R = (2/\lambda)\{V^2/(d+k)\}(h/R_s)\sin\theta \ \sin i. \tag{7}$$

Assume h is 1 km because it covers over 90% of landmass.

3) Polynomial f_R Model Errors

Polynomial f_R model is the cross track quadratic model for f_R. Main across track variation comes from $1/R_s$ dependence. Thus, the quadratic approximation is:

$$1/R_s = 1/(R_o+r) = (1/R_o)(1+r/R_o)^{-1} \cong 1/R_o - r/R_o^2 + r^2/R_o^3 - \cdots\cdots \tag{8}$$

, where R_o is slant range at mid swath and r is the slant range variation relative to swath center: $r=\{(swath\ width)\times sin\ i\}/2$ and R_s is (R_o - r). Thus the relative error (δR_E) in $1/R_s$ is $\{\delta(1/R_s)/(1/R_s)\}$, where $\delta(1/R_s)$ is real estimation error: $\delta(1/R_s) = 1/R_s - (1/R_o + r/R_o^2 + r^2/R_o^3)$. f_R in the case of $1/R_s$ dependence[17] is:

$$f_R = (2/\lambda R_s)\ [V/\{(1+k/d)^{0.5}\}]^2. \tag{9}$$

Then, the f_R error (δf_R) due to polynomial f_R model error is:

$$\delta f_R = f_R \times \delta R_E . \tag{10}$$

4) f_R Change over Azimuth Block

f_R is evaluated at the center of azimuth processing block, and then used for whole processing block. Phase and location errors at block edges are corrected, but focus error cannot be. The azimuth processing block size (A_b) should be $\rangle$ $2\times(interpolator\ length)$ for reasonable computational efficiency. f_R comes from slant range variation (δR_s). Then,

$$\delta R_s = (A_b/2) \times sample\ size = (A_b/2) \times \{c / (2\times A_R)\} \tag{11}$$

, where A_R is Analog to Digital Converter (ADC) rate and c is light velocity. Therefore, f_R error due to f_R change over azimuth processing block is:

$$\delta f_R = (\delta R_s / R_s) \times f_R. \tag{12}$$

2.2. Range Defocus

1) RCM Correction Errors

In addition to the popular range-Doppler approach, a number of accurate algorithms for stripmap SAR processing have been proposed in recent years[18]. These include the chirp scaling algorithm[19] and the range migration algorithm[11]. The range migration algorithm in particular is well suited to dealing with large range migration.

This error is related to the error in f_R. Range migration is $\sim \{\lambda (f_D^2 - f_{DC}^2) / 4f_R\}$, where f_D is Doppler frequency and is fixed by processor and error comes from f_R estimation error, and f_{DC} is the Doppler center frequency.

Maximum $(f_D^2 - f_{DC}^2)$ = Maximum $(f_D^2) = (B_{ap}/2)^2$, where B_{ap} is the azimuth processing bandwidth. Then,

$$\text{Maximum RCM} = \{\lambda/(4f_R)\}(B_{ap}/2)^2. \quad (13)$$

Error in RCM = Error in f_R = Error in slant range. Therefore, Error is $\sim \delta R_s$. Then, the RCM correction error (δRCM) due to f_R mismatch is:

$$\delta RCM = (\delta R_s/R_s)\{\lambda/(4f_R)\}(B_{ap}/2)^2. \quad (14)$$

If yaw steering is not perfect, then $f_{DC} \neq 0$: therefore,

$$\delta RCM = \frac{\delta R_s}{R_s}\frac{\lambda}{4f_R}\{(\frac{B_{ap}}{2} + f_{DC})^2 - f_{DC}^2\}. \quad (15)$$

2) Range Doppler Dispersion

Jin and Wu[8] introduced the concept of SRC in the context of handling cases of severe range walk. It was extended by Schmidt[9] who investigated methods of implementation and multi- look processing. Phase error, if SRC applied, is of form:

$$\delta\varphi = \sim \frac{\pi R_s c}{2}\frac{\{(f_{DC}+0.5B_{ap})^2 - f_{DC}^2\}B_p^2}{V^2 f_c^2 (B_p + f_c)} \quad (16)$$

, where f_c is carrier frequency and B_p is pulse bandwidth. Such errors have less effect than other phase errors since they only affect the azimuth focus for the edges of the range bandwidth.

2.3. Noise Type Errors

1) Interpolation Error

Interpolations are used at 3 processing steps: RCM correction, azimuth deskew, and range resample. A sinc interpolation used to interpolate band-limited data with a uniform spectrum gives a mean square error (δI): 5 points sinc interpolation is 0.012, 7 is 0.006, and 9 is 0.003. Thus Root Mean Square (RMS) error (δI_E) due to interpolation is:

$$\delta I_E \fallingdotseq \delta I \times (N_s)^{0.5} \quad (17)$$

, where N_s is the number of samples. This looks like a noise error. This is independent for each look, averaged in multilook, and then reduced by $1/(number\ of\ looks)^{0.5}$.

2) Computer Truncation Error

Usually we use FFT and IFFT to perform the range and azimuth compression. We assume that our correlator uses a 32-bit CPU using IEEE format. It stores data of 2^{22} bit precision. After each operation, there is an error of 1/2 bit in 2^{22}, an error (δT) of 1 in 10^7. Therefore, RMS error (δT_C) due to computer truncation is:

$$\delta T_C \fallingdotseq \delta T \times (N_e)^{0.5} \quad (18)$$

, where N_e is the number of errors.

2.4. Location Error

Along track displacement (y) from zero Doppler is $\sim f_{DC}/f_R$ in time and is $(f_{DC}/f_R)V_g$ in meters, where V_g is the ground velocity. Therefore,

$$\delta y = V_g (f_{DC}/f_R^2)\, \delta f_R. \quad (19)$$

The orbit errors appear directly as location errors (along and across tracks). The orbit altitude error produces an across track error of $\delta R/\tan I$.

Ⅲ. Simulation & Discussion

The E-SAR processor is the primary image-generating component of E-SAR. Fig. 1 is used

for the performance analysis of the E-SAR processor. The E-SAR parameters and requirements used for simulation are shown at Table 2. Its operation mode is stripmap mode and its swath number is variable from Swath Width number (SW) 1 to SW20, depending on incidence angle, but its swath width is same. It uses on-board Global Positioning System (GPS) receivers for orbital estimation. It is assumed that observation is carried out every 10 seconds and 5 observations are used.

The worst case for E-SAR processor is at SW1 (near field) or SW20 (far field). Then, we can calculate the error values to those two cases among SWs. There are results from table 3 to 6.

The phase error due to f_R change over azimuth block at SW1 is at the design target limit because that of the phase error is $\pi/8$ (22.5°). But an error of 25.32° produces an IRF broadening of 0.6%, then it is acceptable provided there are not several such contributions.

Table 2. Parameters and requirements of the E-SAR

Contents		Values	Unit
Earth radius		6370	km
Satellite height		618	km
Carrier frequency		9.65	GHz
Satellite velocity		7553	m/s
Ground velocity	SW1	6883	m/s
	SW20	6851	m/s
Wave length		0.0311	m
Incidence angle		15~51	degree(°)
Doppler center frequency	SW1	1214	Hz
	SW20	3639	Hz
Pulse bandwidth	SW1	65	MHz
	SW20	25	MHz
Azimuth processing bandwidth		2551	Hz
Light velocity		3×10^8	m/s
ADC rate		60	MHz
Azimuth processing block size		115	samples
Synthetic aperture duration		0.682~0.966	s
GPS accuracy		± 20	m
Swath width		33	km
f_R change over azimuth block		$\leq \pi/8$	radians
Yaw steering error		± 0.6	°
Impulse Response Function (IRF) broadening		< 1	%

Table 3. Azimuth focus errors

Processing errors	Symbol	Unit	Value	Remark
Position errors	δR	m	±9	
Orbital estimation errors	$\delta\varphi$	°	0.1608	SW1
	$\delta\varphi$	°	0.2234	SW20
Terrain height errors	δf_R	Hz/s	0.05	SW1
	δf_R	Hz/s	0.32	SW20
	$\delta\varphi$	°	1.047	SW1
	$\delta\varphi$	°	13.437	SW20
Polynomial f_R model errors	$\delta\varphi$	°	0.032	SW1
	$\delta\varphi$	°	0.247	SW20
f_R change over azimuth block	δf_R	Hz/s	1.21	SW1
	δf_R	Hz/s	0.57	SW20
	$\delta\varphi$	°	25.32	SW1
	$\delta\varphi$	°	24.11	SW20

Table 4. Range focus errors

Processing errors	Symbol	Unit	Value	Remark
Range Doppler dispersion(with yaw steering error of 0.6°)	$\delta\varphi$	°	6.66	SW1
	$\delta\varphi$	°	3.3	SW20

Table 5. RCM correction errors

Processing errors	Symbol	Unit	Value	Remark
RCM errors (with perfect yaw steering)	δRCM	m	5.14×10^{-4}	SW1
	δRCM	m	5.18×10^{-4}	SW20
RCM errors (without perfect yaw steering : then 0.6° yaw steering error)	δRCM	m	1.5×10^{-3}	SW1
	δRCM	m	3.5×10^{-3}	SW20

Table 6. Noise type and location errors

Processing errors	Symbol	Unit	Value	Remark
Mean square error for number of interpolation points				
- 5 points	δI_E	dB	0.13	
- 7 points	δI_E	dB	0.064	
Computer truncation error	δT_C		2×10^{-6}	negligible
Location error due to f_R error	δy	m	1.21	SW20

The error can be reduced by using a smaller block size. In computer truncation errors, dominant calculation is FFT. Each FFT has about 50 steps with two errors per step (the operation+twiddle table). There are 2 forward and 2 backward FFT[17]: about 400 errors, then RMS

error=2×10^{-6}. Table 7 summarizes the worst case error values in the various categories. To assess these it is necessary to compare with other similar errors, to consider how they can be combined with such errors, and to estimate their impact on system performance parameters such as the IRF.

Note that the dominant error comes from terrain height variations. The range quadratic phase error is from range dispersion. This has less effect than other phase errors. The worst case IRF broadening (maximum yaw steering error) is still $<$ 1%. f_R change over azimuth block is a little bigger than criteria ($\pi/8$), so the block size should be reduced for single look. In the case of multi-look, the synthetic aperture time is reduced by *1/(the number of looks)*. Therefore, the phase error is reduced by *1/(the number of looks)*^{2}. The noise type error is 0.13㏈ if 5 points interpolation used.

Table 7. Processing error values in the worst case

Processing errors	Unit	Contribution	Worst case value	SW No
Azimuth focus (f_R) errors				
- Orbital estimation errors	°	Qa	0.2234	SW20
- Terrain height errors	°	Qa	13.437	SW20
- Polynomial f_R model errors	°	Qa	0.247	SW20
- f_R change over azimuth block	°	Qa	25.32	SW1
Range focus errors				
- Range Doppler dispersion	°	Qr	6.66	SW1
RCM correction errors				
- f_R mismatch : with yaw steering	m	Br	5.18×10^{-4}	SW20
- f_R mismatch : without yaw steering	m	Br	3.5×10^{-3}	SW20
Noise type errors				
- Interpolation : 5 points	㏈	N	0.13	
- Truncation	㏈	N	2×10^{-6}	
Calibration errors		system error		
Location errors				
- Orbit: along track	m	a	9	
- Orbit: across track	m	r	9	
- Orbit : altitude (across track)	m	a	33.8	SW1
- f_R error	m	a	1.21	SW20

cf.) Q: quadratic phase error, B: broadening due to mislocation, N: noise, a: along track, r: across track.

Ⅳ. Conclusion

This paper started to identify the main sources of SAR processor errors and considered errors that are due to imperfections in the algorithms selected, or in their implementation. It suggested the analysis technique for principal performance of the space-based SAR processor using RDA: equations, input and output parameters, and their relationship. Also, simulation has been performed to the E-SAR processor. The contribution to overall system performance budget degradation is small except for terrain height variation induced IRF broadening. But this broadening is still well within acceptable limit. The dominant location errors come from orbit errors and the computation errors are much less at a few tenths of a pixel. They are small enough for automated image alignment techniques to work even in interferometric applications.

Therefore, this paper has summarized and proposed the overall works related to the principal performance analysis of the space-based SAR processor using RDA. Our approach can provide the effective and practical technique for analyzing the principal performance of the space-based SAR processor.

REFERENCES

[1] Charles Elachi, T. Bicknell, Rolando L. Jordan, and Chialin Wu, "Spaceborne synthetic aperture imaging radars: Applications, techniques, and technology," *Proc. IEEE*, vol. 70. no 10, pp. 1174-1209, Oct. 1982.

[2] Leopold J. Cantafio, *Space-based Radar Handbook*, Norwood, MA : Artech House, ch. 1, 2, 1989.

[3] Michael Y. Jin, "A Doppler centroid estimation algorithm for SAR systems optimised for the

quasi-homogeneous source," *JPL publication* 89-9, Oct. 1989.

[4] Michael Y. Jin, "Optimal Doppler centroid estimation for SAR data from a quasi-homogeneous source," *IEEE Trans. Geosci. Remote Sensing*, vol. GE-24, no. 6, pp. 1022-1025, Nov. 1986.

[5] S. Norvang Madsen, "Estimating the Doppler centroid of SAR data," *IEEE Trans. AESS*, vol. AES-25, no. 2, pp. 134-140, Mar. 1989.

[6] Alberto Moriera, Rolf Scheiber, Josef Mittermayer, and Rainer Spielbauer, "Real-time implementation of the extended chirp scaling algorithm for air- and spaceborne SAR-processing," *Proc. IGARSS 95*, vol. 3, pp. 2286-2288, 1995.

[7] Alberto Moreira, "Real-time Synthetic Aperture Radar(SAR) processing with a new subaperture approach," *IEEE Trans. Geosci. Remote Sensing*, vol. 30, no. 4, pp. 714-722, July 1992.

[8] Michael Y. Jin and Chialin Wu, "A SAR correlation algorithm which accommodates large-range migration," *IEEE Trans. Geosci. Remote Sensing*, vol. GE-22, no. 6, pp. 592-597, Nov. 1984.

[9] Schmidt, A. R., "Secondary range compression for improved range/Doppler processing of SAR data with high squint," M. Sc. Thesis, Department of Electrical Engineering, U. B. C., Sep. 1986.

[10] Knut Eldhuset, "A new fourth-order processing algorithm for spaceborne SAR," *IEEE Trans. AESS*, vol. 34, no. 3, pp. 824-835, July 1998.

[11] C. Cafforio, C. Prati, and E. Rocca," SAR data focusing using seismic migration techniques," *IEEE Trans. AESS*, vol. 27, no. 2, pp. 194-207, Mar. 1991.

[12] Richard Bamler, "A comparison of range-Doppler and wavenumber domain SAR focussing algorithms, *IEEE Trans. Geosci. Remote Sensing*, vol. 30, no. 4, pp. 706-713, July 1992.

[13] Walter G. Carrara, Ron S. Goodman, and Ronald M. Majewski, *Spotlight Synthetic Aperture Radar : Signal Processing Algorithms*, Boston : Artech House, ch. 12, 1995.

[14] Charles Elachi, *Spaceborne Radar Remote Sensing : Applications and Techniques*, New York : IEEE press, ch. 4, 1988.

[15] Cumming I. G. and J. R. Bennett, "Digital processing of SEASAT synthetic aperture radar data," *IEEE International Conference on Acoustics, Speech and Signal Processing*, Washington, D. C.,April, 1979.

[16] F. H. Woong and I. G. Cumming, "Error sensitivities of a secondary range compression algorithm for processing squinted satellite SAR data," *Proc. IGARSS 89*, vol. 4, pp. 2584-2587, 1989.

[17] John C. Curlander, and Robert N. McDonough, *Synthetic Aperture Radar : Systems & Signal Processing*, New York : John Wiley & Sons, Inc., pp. 554-591, 1991.

[18] Jasper M. Horrell and Mike R. Inggs, "Low frequency range-Doppler SAR processing without secondary range compression," *Proc. COMSIG 98*, South African, pp. 109-114, 1998.

[19] R. Keith Raney, H. Runge, Richard Bamler, Ian G. Cumming, and Frank H. Wong, "Precision SAR processing using chirp scaling," *IEEE Trans. Geosci. Remote Sensing*, vol. 32, no. 4, pp. 786-799, July 1994.

홍 인 표(In-Pyo Hong) 정회원
한국통신학회 논문지 Vol. 27, No. 4B, 2002년 4월 참조